PASSENGER EFFECTS ON ELECTROMAGNETIC PROPAGATION PREDICTION INSIDE AIRPLANE FUSELAGES

Mennatoallah M. Youssef
Old Dominion University
Advisor: Dr. Linda L. Vahala

Abstract

The focus of this research is to determine how passengers will effect power propagation. Passenger models were added to the fuselage environment. They were assigned various material characteristics. It was determined that passengers tend to adversely effect power propagation. More detailed systems are currently being tested with results to follow soon.

Introduction

In today's industrialized world, wireless networking is becoming more widespread. Companies, universities, and neighborhoods are equipping themselves with this revolutionary advancement. The average person can be connected to any network from almost any remote location.

What makes wireless networks so attractive is their easy accessibility. Particularly in today's society, an individual is dependent on the Internet for a multitude of tasks ranging from paying bills to entertainment. As this technology advances, there will be more uses for wireless networks. They will be heavily adopted more so into everyday life. [9,10]

Since wireless networks have existed for the past decade, there is already been a move to implement them in aircraft cabins. European Airline Lufthansa has already started trials in their charter planes the Condor ; they have recently gained approval to install a wireless radio connection in a Boeing 747-400 provided it meets special structural criteria. [5]

Competition from other international airlines is pushing the Federal Aviation Administration (FAA) to reexamine its position. They are concerned with wireless networks interfering with onboard communications systems. But the tremendous boom in the wireless network industry, with revenue expected to be $83 million from wireless technology, has led to the FAA predicting that the approval of in-flight systems may occur in another year or two. [5]

Implementing a wireless system on airplanes hasn't been tested in the cabin extensively in the United States. Airlines are financially constrained after September 11th and physically testing can be done but it is both expensive and time consuming. Another problem is that airplane models vary from; company-to-company, type, and year produced. Airline companies often fit internal configurations to their personal specifications. Therefore it is cost prohibitive to physically test each configuration in a commercial fleet.
Modeling and simulation could be applied to the various airplane classes to produce a general idea of wireless network design and optimum placement of network components. Simple models of the individual aircrafts can be used to examine the effects of wireless networks in the fuselage. Thus an electromagnetic propagation prediction tool can be used to simulate the environment in an aircraft cabin.

Modeling and simulation is advantageous in many ways; it can decrease the time and cost associated with physical testing while providing quick parameter change on demand. This would provide an erudite method of examining the electromagnetic propagation of the signals.

There are multiple electromagnetic propagation prediction tools on the market. Wireless Insite by Remcom Inc. will be used to test whether it is an effective and accurate method of simulation of a wireless communication system within aircraft cabins. To verify the effectiveness of Wireless Insite a simulation environment will be created on the basis of an experimental study done by the Embry Riddle Aeronautical University.

Signal Propagation Effects

Signals propagating from any of these standards face problems that wired networks do not. When a signal propagates from the transmitter to the receiver there is a possibility of multipath effects. The receiver picks up reflected, diffracted, and attenuated copies of the transmitted signal if there is no line of sight path due to surrounding objects. Reflection occurs when a wave meets a boundary and changes directions; diffraction is when the wave bends around the boundary or obstacle.[11]

When a signal reflects off an obstruction and then travels to the receiver, the signal is delayed and has traveled a longer distance to reach the receiver. Thus the signal has lost energy from the reflection. The multiple waves that are traveling recombine at the receiver. They can modify the waveform and consequently affect the signal quality at the receiver. Therefore multipath can be dependent on the objects in the WLAN environment, the transmitter-receiver distance, line of sight, and radio technology. Figure 1 depicts a WLAN system in which eaves are traveling from two transmitters to two possible receivers. The letter “D” in the diagram represents where the signal has diffracted and “R” represents where the signal has reflected off the surface. A signal can undergo multiple diffractions and reflection before it reaches the receiver. [11]

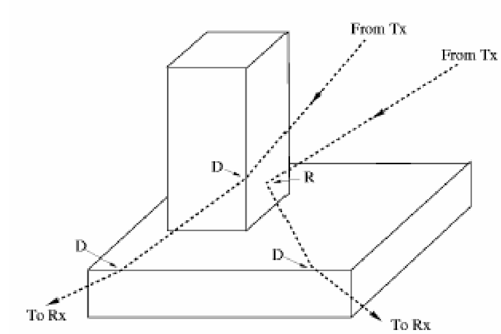

Figure 1: Example of Diffraction and Reflection of Signals off an Arbitrary Building [2]

Diffraction and reflection are going to play a key role when examining the power propagation in the fuselage. When WLAN’s are used in an environment, there is desire to have very few obstruction so that line of sight can be maximized. A fuselage is more crowded than the average environment. It is composed of an Aluminum alloy, which will account for some signal reflections. Another factor is the number of people that are in the fuselage. The signal can also decay quite rapidly with distance in this setting. Therefore understanding how electromagnetic waves travel in complex environments has been the focus of many studies. [6,11]

Electromagnetic Modeling

There are many available codes for use in electromagnetic modeling. Numerical techniques such as Method of Moments and Finite element often find it difficult to solve for electromagnetic propagation in a complicated geometry and use very high memory and CPU processing times. The Finite Difference Time Domain [FDTD] method is more suitable to the stated application. [7]

FDTD uses Maxwell’s time dependent curl equations show below in Equation 1. The space and time derivatives are calculated in central difference equation form. The area modeled is represented as two grids [Yee’s lattice]; one grid is for electric field calculation and the other for the magnetic field. The electric field and magnetic field are alternatively computed. For example the

Electric field at time t is used to calculate the magnetic field at time $t + \tau$ where, is the time increment. [7]

The FDTD also allows for each section of the lattice to be assigned μ, ε, and σ which describe the parameters of the media.[7]

$$\nabla \times \mathbf{E} = -\mu \frac{\partial \mathbf{H}}{\partial t}$$

$$\nabla \times \mathbf{H} = \sigma \mathbf{E} + \varepsilon \frac{\partial \mathbf{E}}{\partial t}$$

Equation 1: Maxwell's Time Dependent Curl Equations [7]

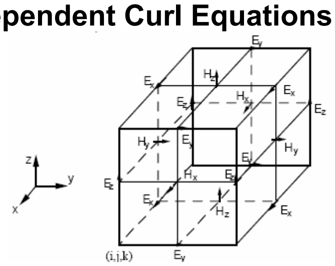

Figure 2: Yee's Lattice[7]

Creating the Simulation Environment

Software

The foundation of the simulation highly depends on the accuracy put forth in recreating the environment that is to be simulated. The first step is to create the fuselage for Wireless Insite. Wireless Insite (WI) and XGTD .

The method of propagation used is the shooting and bouncing ray method (SBR). SBR uses geometrical optics to trace the rays. Numerous rays are shot at an object, and then their movement traced according to geometrical optics. When the SBR paths have been traced, a path is recorded. [2]

Fast 3D Urban Model (FUM) is the first model tested. This model uses the same method described above but in addition it also takes into account the tops of low lying objects around the transmitter and receivers. The FUM does not use a full 3D trace; Fast 3D means that the vertical components of some objects are considered in the calculations. FUM incorporates the heights of other objects when making calculations. Basically it is used if there are many objects of varying heights that could possibly have ray paths that affect the calculations. To account for the effects, SBR and multiple image methods in 3D geometry are used. The SBR is used for calculation in the horizontal plane; image method is used for ground reflection and ray path with less than 2 interactions. SBR main purpose is to find the paths of the ray. The program then calculates whether the rays have diffracted, passed over or intersected a boundary object. Depending on the situation above, paths are constructed and the most probable is obtained. FUM incorporates the heights of other objects when making calculations. It is generally used if there are many objects of varying heights that could possibly have ray paths to affect the calculations. [2]

For the FUM to be acceptable, two assumptions must be made. The first assumption is that the distance that the path is shifted vertically is small compared to the path length. This will be valid when the horizontal distance between the transmitter and receiver is greater than the vertical distance. The second assumption made is that shape of an object is not intricate. Since the vertical plane calculation is simplified, a complex shaped would take more paths, which would not be accounted for. [2]

The second model used is the Full 3D Method (FM). Of the two models, FM is recommended for indoor simulation and places no constraint on the object shape. It is the only model that allows for transmission through surfaces. Thus is most applicable for indoor environments. The FM combines SBR and MI ray tracing. MI is used when a path has three or fewer interactions. Paths with more than three interactions are found with SBR method. The thorough use of both methods produces a 3D model that takes into account many parameters. It is expected to deliver the most accurate results of the three models.

Electric Field Calculations

In free space the electric field [with direction of ϕ and θ and distance of r] is defined as follows:

$$\boldsymbol{E}(r,\theta,\phi) = \left(A_\theta(\theta,\phi)\hat{\boldsymbol{e}}_\theta + A_\phi(\theta,\phi)\hat{\boldsymbol{e}}_\phi\right)\frac{e^{-j\beta r}}{r}$$

Equation 2

With

$$A_\theta(\theta,\phi) = \sqrt{\frac{P_T\eta_0}{2\pi}}g_\theta(\theta,\phi)$$

$$A_\phi(\theta,\phi) = \sqrt{\frac{P_T\eta_0}{2\pi}}g_\phi(\theta,\phi)$$

$$g_\theta(\theta,\phi) = \left|G_\theta(\theta,\phi)\right|^{1/2} e^{j\psi_\theta}$$

$G_\theta(\theta,\phi)$ is the θ component of the gain of the transmitting antenna. Ψ_θ is the relative phase of the θ component of the far zone electric field. The same definition holds true for the ϕ component. Bandwidth is defined as a function of frequency and speed of light.

$$\beta = \omega/c$$

P_T is the time-averaged power radiated from transmitter with r being the field point distance from transmitter.

The incident electric field when reflected is not always parallel or perpendicular to the plane of incidence. The field is a combination of both. The reflected field is defined by the components of the reflected electric field that is parallel and perpendicular to the reflected plane. The following variables used are defined as $E_\parallel^r$ is the electric field of the reflected wave parallel to plane of incidence, $E_\perp^r$ is the electric field of the reflected wave perpendicular to the plane of incidence, $R_\parallel$ is the reflection coefficient of the plane parallel to the plane of incidence, and $R_\perp$ is the reflection coefficient of the plane perpendicular to the plane of incidence.

$$\begin{pmatrix} E_\parallel^r \\ E_\perp^r \end{pmatrix} = \begin{pmatrix} R_\parallel & 0 \\ 0 & R_\perp \end{pmatrix}\begin{pmatrix} E_\parallel^i \\ E_\perp^i \end{pmatrix}$$

Equation 3

Where,

$$E_\perp^i = \hat{\boldsymbol{e}}_\parallel \cdot \boldsymbol{E}^i$$

$$E_\parallel^i = \hat{\boldsymbol{e}}_\parallel \cdot \boldsymbol{E}^i$$

$$\hat{\boldsymbol{e}}_\parallel = \boldsymbol{k}\times\hat{\boldsymbol{e}}_\perp / |\boldsymbol{k}\times\hat{\boldsymbol{e}}_\perp|$$

$$\hat{\boldsymbol{e}}_\perp = \boldsymbol{k}\times\hat{\boldsymbol{n}} / |\boldsymbol{k}\times\hat{\boldsymbol{n}}|$$

$$\hat{\boldsymbol{e}}'_\parallel = \boldsymbol{k}'\times\hat{\boldsymbol{e}}_\perp / |\boldsymbol{k}'\times\hat{\boldsymbol{e}}_\perp|$$

The vector **k** is the direction of propagation of incident filed and **k'** is the direction of propagation of the reflected field.
Therefore the reflected field is defined in Equation 4.

$$\boldsymbol{E}^r = \hat{\boldsymbol{e}}'_\parallel \cdot E_\parallel^r + \hat{\boldsymbol{e}}_\perp \cdot E_\perp^r$$

Equation 4: Electric Field for Single Reflection

Fuselage Models

To validate EM power propagation predictions inside aircraft cabins, it was necessary to compare the simulation to an experimental study. Embry-Riddle Aeronautical University tested WLAN (Wireless Local Area Networks) performance in four airplanes (B747-400, B767-300, B777-200, & Airbus A320-200) The fuselages examined are from the Boeing family, the Airbus model was not included in this study.

Two fuselages models were created for each plane; they will then be compared. The first model was used in previous research; it an empty hollow fuselage. The second model includes seats, galley, lavatories, windows, doors, and luggage compartments. The empty models were created using AutoCAD whereas the second set were created in Solidworks®. Solidworks® provides an easier venue for drawing and modeling accurately. The models are shown below in the WI program:

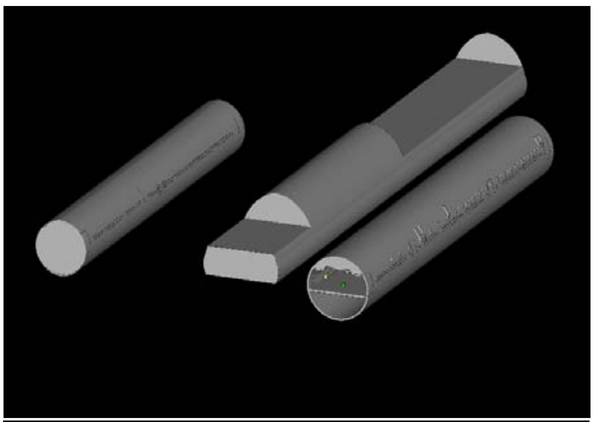

Figure 3: Boeing Models

Figure 4: Internal Boeing Model of B767

<u>Network Components Representation</u>

After the Solidworks® drawings were imported, they are assigned material properties. For simulation purposes it was assumed that the fuselage metal was a Perfect Electrical Conductor (PEC). Various coefficient types such as roughness, conductivity, permittivity, and thickness are also incorporated. Reflection may play a role when collecting results. [2]

The waveform for each antenna was also created. The program offers two choices of waveforms, wideband and narrowband. Narrowband was chosen because the bandwidth is less than the frequency of operation.

Four different antennas were needed to model the 11a and 11b standards. Each antenna is associated with a waveform. For the transmitters, a linear dipole antenna was used for both standards with the individualized waveform, antenna length, gain, polarization, and transmission line loss. The WI database provided the antenna basics for the transmitter. WI also generates the antenna patterns (visual depiction of the E-plane and the H-plane on different axes). The receiver antennas were not generated by the WI database since they are integrated antennas. An antenna format file that designates gain, polarization, and transmission line loss was created from the antenna pattern of the receiver that was obtained from the FCC Website. The antenna was then imported and assigned to the receiver. Again each system antenna had the same specifics. [2]

Transmitter and receiver creation and placement was the next step. To determine the accuracy of the data compared to experimental results, it was important to place the transmitters and receiver in the same location and orientation as the experimental setup. Transmitters needed the following properties to operate, coordinate system elevation type, rotation, waveform, antenna type, radiated power, and rotation about each plane in the xyz system. The height, rotation about the axis, and orientation differed for each plane. Receivers were easier to place. The receivers were laid as a strip on the left portion of the fuselage.

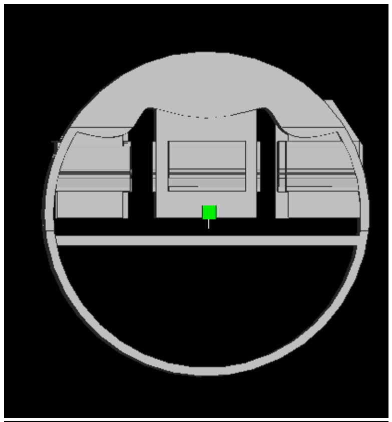

Figure 5:Transmitter placements in the fuselage

Access Points	ORiNOCO AP 2000
Standard	802.11a & 802.11b
Antenna Type	Two omnidirectional (11a) Linear dipole (11b)
Antenna Gain	5.0 dBi (11a) 2.0dbi (11b)
Output Power	802.11a:17dBm 802.11b: 18dBm
Polarization	Vertical

Table 1: Simulation Parameters

Power Calculation

Power calculations differed in each environment. The received power is defined as the total power received by the receiver antenna. It is measured in units of dBm, which is a measure of decibels relative to 1mW of power (0 dBm = 1mW).
The time averaged received power for Wireless Insite (P_R) is calculated by the following relationships. The received power is calculated by summing the individual power in the electric field without the phase information. [2]

$$P_R = \sum_{i=1}^{N_p} P_i$$

where $N_P =$ number of paths, $P_i =$ time averaged power (in watts) of the ith path.

$$P_i = \frac{\lambda^2 \beta}{8\pi^2 \eta_0} \left| E_{\theta,i} \; g_\theta(\theta_i,\phi_i) + E_{\phi,i} \; g_\phi(\theta_i,\phi_i) \right|^2$$

where $\lambda =$ wavelngth, $\eta_0 =$ impedance of free space, $\beta =$ overlap of frequency spectrum of the transmitted waveform. $\mathrm{E}_{\theta,i}$ and $E_{\phi,i}$ are the $\theta -$ and $\phi -$ components of the electric field of the ith path at the receiver path. θ_i and ϕ_i is the arrival direction, $g_\theta(\theta_i,\phi_i) = \left|G_\theta(\theta_i,\phi_i)\right|^{1/2} e^{i\psi}$ where G_θ is the $\theta -$ component of the receiver antenna gain and ψ the relative phase of the $\theta -$ component of the far zone electric field. Similarly for g_ϕ with θ Ä ϕ. β is defined as

$$\beta = \frac{\int_{f_T - B_T/2}^{f_T - B_T/2} S_T(f)\, S_R(f)\, df}{\int_{f_T - B_T/2}^{f_T - B_T/2} S_R(f)\, df}$$

where f_T and B_T are the center frequency and bandwidth of the transmitted waveform, $S_T(f)$ is the frequency spectrum of the transmitted waveform and $S_R(f)$ is that for the received waveform.

Human Models

Human models were then added to the system to examine their effects. The idea of modeling is to create a simple system. Therefore humans were created as simple blocks placed in the fuselage as shown in Figure 6. They were assigned as fresh water, muscle, and bone. The simulation was run for each of these material properties. The permittivity and conductivity for each material is represented in Table 2:

Material	Permittivity	Conductivity[S/m}
Skin	40	1.4
Muscle	50	2
Bone	18	.6
Fat	4	.08

Fresh Water	81	.2

Table 2: Material Properties

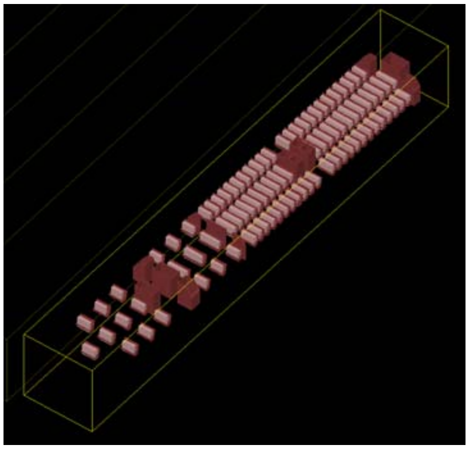

(a)

(b)

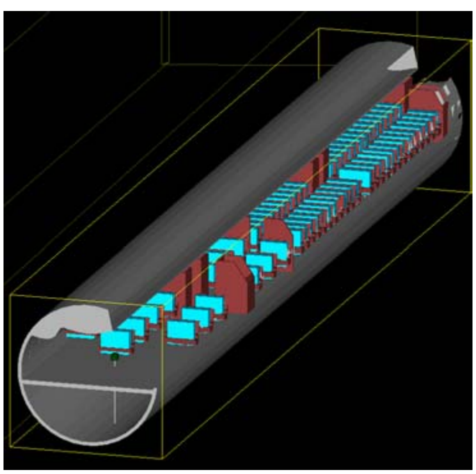

(c)

Figure 6: Human Blocks Placed in Fuselage with three different views

Material assignment is very important for the fuselage. Figure 7 shows the effects on power levels if a “wall” of each of the materials was created. Receiver one was place directing in front of the wall and receiver two was placed behind the material. Notice that muscle has a significant drop from one receiver to the other.

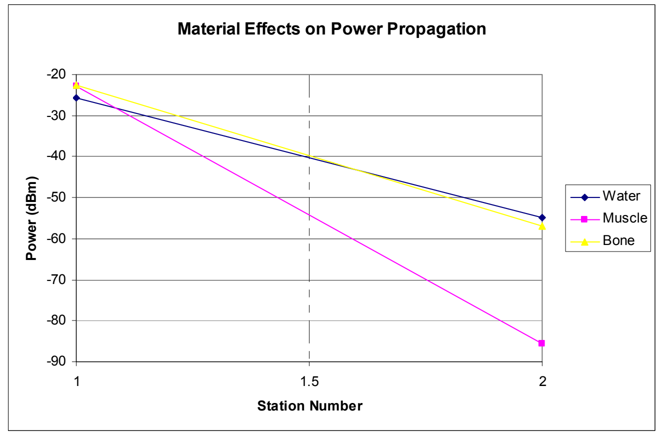

Figure 7: Material Effects on Power Propagation

When changing the material composition to a perfect electrical conductor [PEC], we can see that none of the power is transmitted to the second receiver. The waves are reflected off the surface.

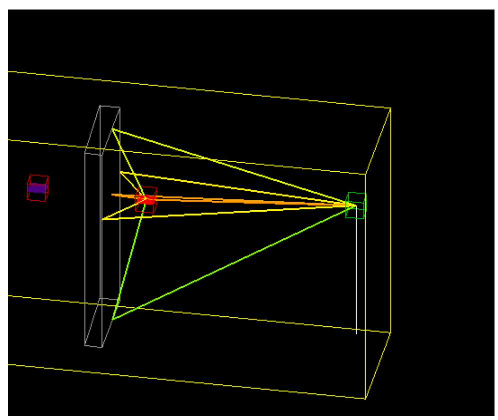

Figure 8: Reflection of Waves for a PEC

Results

The predicted results were graphed with the measured data for comparison. The graphs for the 802.11a standard are shown below. In addition, the Mean Absolute Error (MAE) and Root Mean-Squared Error (RMSE) were calculated for both sets of data. The equations for the MAE and RMSE are shown below. Where P_M is the measured power without passengers, P_P is the measured power with passengers, and N is the number of data points collected.

$$MAE = \frac{\sum \left| P_M - P_P \right|}{N}$$

$$RMSE = \sqrt{\frac{\sum \left(P_M - P_P \right)^2}{N}}$$

The tables are shown below:

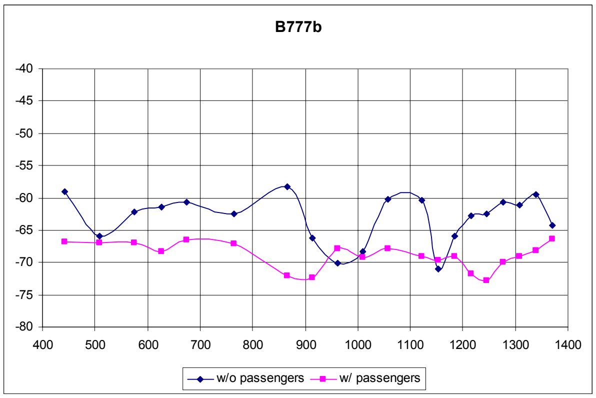

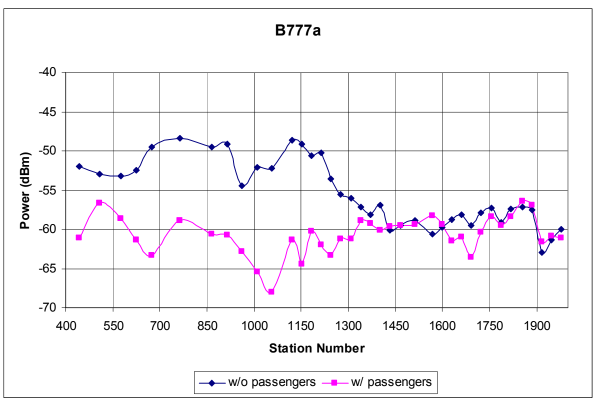

Plane	MAE	RMSE
777a	5.530	7.450
777b	6.127	7.018

Conclusion

Passenger models were added to the fuselage environment. Material composition of humans is an important factor to consider in simulation environments. Passengers tend to change the propagation path of a signal. They also increase diffraction and reflection. Overall passengers adversely effect power propagation.

Continuing Work

The next step is to incorporate more realistic looking models. The model will be assigned both muscle and bone as its material composition. A model was obtained and is currently being examined to determine accuracy. Figure 9 depicts the new model. This representation may vary from previous results obtained due to its curvature differences. Results are expected by the end of the semester.

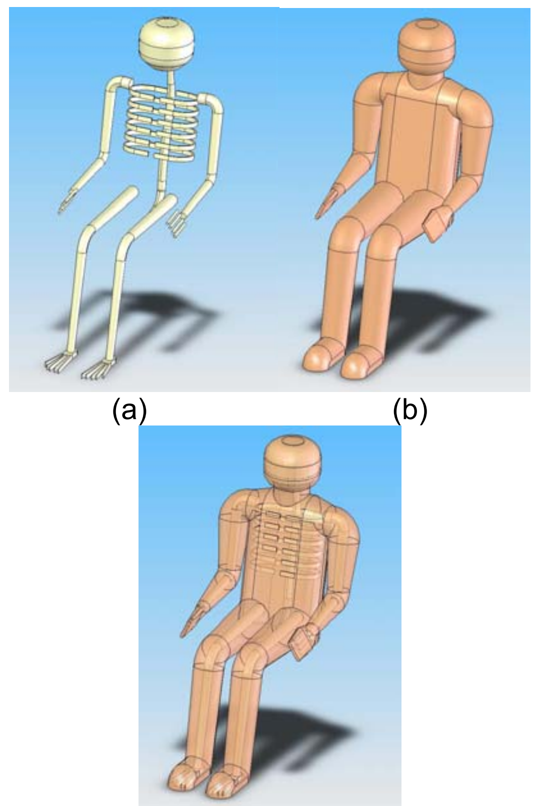

(a) (b)

(c)

Figure 9: Detailed Passenger Models
(a) Skeleton (b) Muscle
(c) Combined model

References

[1] Whetten, F.; Soroker, A.; Whetten, D. 802.11 Wireless Network Performances within Aircraft Cabins. Embry-Riddle Aeronautical University: 2003.

[2] Remcom Incorporated. Wireless Insite User's Manual 2.0.5 December 2004

[3] Tanenbaum, Andrew. Computer Networks. New York: Prentice Hall PTR, 2003

[4] Carlson, Bruce, Paul Crilly, and Janet Rutledge. Communication Systems. New York: McGraw Hill, 2001

[5] Ramsey, James, "Wireless Undeterred." http://avionicsmagazine.com/cgi/av/show_mag.cgi?pub=av&mon=0204&file=0204wireless.htm 4 February 2004. 12 January 2005

[6] W.K. Tam and V.N. Tran. Multi-ray propagation model for indoor wireless communications. *Electronics and Communication Engineering Journal*, 32:135–137, Jan 1996.

[7] Damasso, E., Paraboni, A., Protto, F., "Indoor propagation measurements: application to mobile channel modeling", 8th Int. Conf. on Antennas and Propagation, Edinburgh, UK, March 1993

[8] Yee, K. S.: Numerical solution of initial boundary value problems involving Maxwell's equations in isotropic media. *IEEE* Transactions: Antennas Propagation, Vol. 14, pp 302-307, May 1966.

[9] Rappaport, T.S., Annamalai, A., Buehrer, R.M., and Traniter, W.H.: 'Wireless communications: past events and future perspective', IEEE Communication. Magazine., 50th Anniversary Commemorative Issue, May 2002

[10] Jahn, A.; et al. **:'**Evolution of aeronautical communications for personal and multimedia services' Communications Magazine, IEEE Volume 41, Issue 7, July 2003 Page(s):36 – 43

[11] D. Dobkin. "Indoor propagation issues for wireless LANs." RF Design; www.rfdesign.com, Sep 2002. 12 January 2005.

[12] Homepage. Boeing. April 2, 2005. Boeing. { http://www.boeing.com/flash.html}

[13] Homepage. Federal Communication Commission. April 2, 2005. FCC.{ http://www.fcc.gov/}